11th World Congress on Computational Mechanics (WCCM XI)
5th European Conference on Computational Mechanics (ECCM V)
6th European Conference on Computational Fluid Dynamics (ECFD VI)
E. Oñate, J. Oliver and A. Huerta (Eds)

COMPARATIVE STUDY FOR THE EFFICIENT CONSTRUCTION OF STATISTICALLY SIMILAR RVES: LINEAL-PATH AND MINKOWSKI FUNCTIONALS

LISA SCHEUNEMANN*, DOMINIK BRANDS*, DANIEL BALZANI* AND JÖRG SCHRÖDER*

* Institute of Mechanics, Faculty of Engineering
University Duisburg-Essen
Universitätsstr. 15, 45141 Essen, Germany
e-mail: lisa.scheunemann@uni-due.de , web page: http://www.uni-due.de/mechanika

Key words: Microstructure, Representative Volume Element, FE^2-Method, Dual-Phase Steel, Statistically Similar RVEs

Abstract. Advanced high strength steels, such as Dual-Phase steel (DP steel), provide advantageous material properties for engineering applications compared to conventional high strength steel mainly originating from a ferritic-martensitic microstructure. A way to include these heterogeneities on the microscale into the modeling of the material is the FE^2- method. Herein, in every integration point of a macroscopic finite element problem a microscopic boundary value problem based on the definition of a representative volume element (RVE) is attached. From this representation, high computational costs arise due to the complexity of the discretization which can be circumvented by the use of a statistically similar RVE (SSRVE) showing a lower complexity. For the construction of such SSRVEs, a least-square functional is minimized which takes into account differences of statistical measures evaluated for the real microstructure and the SSRVE. The choice of the statistical measures which are considered in the least-square functional however influences the quality of the SSRVE and on the other hand the computing time required for the construction. Therefore, in this contribution we analyze statistical measures of different type and complexity. We focus on the volume fraction, the spectral density, the lineal-path function and measures based on Minkowski functionals. The performance is checked in virtual tests where the response of the individual SSRVEs is compared with the real target microstructure of a DP steel.

1 INTRODUCTION

As a result of the interaction of microstructural constituents in DP steel, martensitic inclusions embedded in a soft ferritic matrix, higher strength combined with good forma-

bility is observed. In order to incorporate the microstructural mechanical fields directly into a modeling approach, direct micro-macro approaches can be applied (FE^2-method), see e.g.[3]. This two-scale approach attaches a microscopic finite element (FE) problem, represented by a Representative Volume Element (RVE), to every integration point of the macroscopic FE problem. The RVE is typically given by a suitable segment of a real microstructure, which involves complex morphologies due to the underlying microstructure topology of the material and thereby leads to expensive computations. The efficiency of the method can be improved by using Statistically Similar RVEs (SSRVEs), cf.[5], which are characterized by a lower complexity of the morphology, but which are still similar to real microstructures in terms of statistical measures describing the microstructure morphology. These SSRVEs are constructed by the minimization of a least-square functional taking into account suitable differences of statistical measures for the real microstructure and the SSRVE. Here, the statistical measures used play a crucial role. Hybrid approaches utilizing multiple statistical measures have shown to give better results compared to approaches with only one type of statistical measures, cf.[7, 1]. Higher order statistical measures are advantageous to capture important properties of the microstructure, such as connectivity or long range properties. Studies with SSRVEs constructed based on the phase fraction, spectral density and lineal-path function turned out to be able to represent the mechanical response of the real microstructure accurately, however the computation of the lineal-path function, which represents the probability that a line segment of a certain length and orientation is completely located in one phase of the material, lacks computational efficiency. To improve the performance of the optimization procedure, other statistical measures are taken into account. The focus of this work lies on the Minkowski functionals, which are scalar, vectorial or tensorial measures which capture information using surface integrals over a microstructure feature. Here, one tensorial Minkowski functional $\mathcal{W}_2^{0,1}$ is used to capture information on surface orientation and anisotropy. SSRVEs based on the spectral density, lineal-path functional and phase fraction are compared to ones which are constructed based on the Minkowski tensor $\mathcal{W}_2^{0,1}$, spectral density and phase fraction.

2 CONSTRUCTION METHOD FOR SSRVES

The proposed method is based on the assumption that a real, typically non-periodic microstructure, can be replaced by a periodic microstructure, see Fig. 1. A method for the construction in 2D is proposed in [5] and has been extended to 3D in [2]. In this method a least-square functional, taking into account suitable statistical measures computed for the real microstructure and the SSRVE, is minimized. An adequate parameterization for the SSRVE is then given by

$$\boldsymbol{\gamma}^* = \operatorname{argmin}\left[\mathcal{L}(\boldsymbol{\gamma})\right] \qquad \text{with} \qquad \mathcal{L}(\boldsymbol{\gamma}) := \sum_{i=1}^{nsm} \omega_i \left(\mathcal{P}_i^{\text{real}} - \mathcal{P}_i^{\text{SSRVE}}(\boldsymbol{\gamma})\right)^2 \tag{1}$$

with $\mathcal{P}_i^{real}$ and $\mathcal{P}_i^{SSRVE}$ representing an appropriate statistical measure i of the real microstructure and the SSRVE, respectively, and ω_i denoting appropriate weighting factors. The total number of statistical measures is described by nsm and the vector $\boldsymbol{\gamma}$ describes a parameterization of the inclusion morphology.

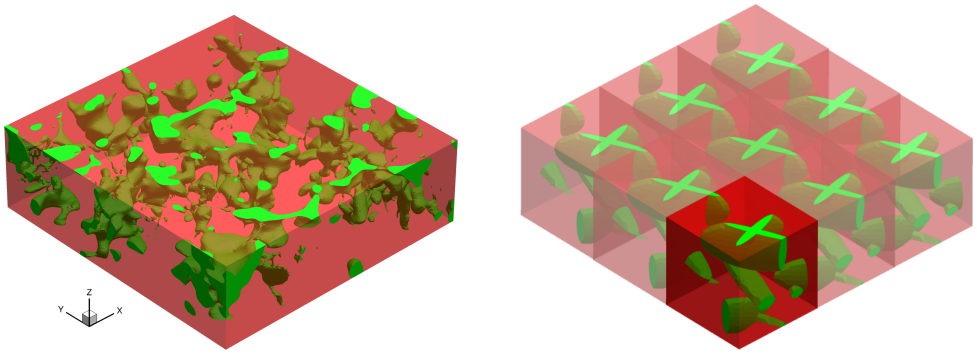

(a) (b)

Figure 1: Schematic illustration of the basic concept, red indicating the matrix phase, green indicating the inclusion phase: (a) usual RVE with arbitrary inclusion morphology and (b) periodic microstructure with SSRVE.

2.1 Statistical Measures

An overview on statistical measures describing the morphology of a single phase in a multiphase material can be found in [4]. In the wide field of statistical descriptors, general information is enclosed in basic, scalar-valued parameters such as the phase fraction, which is defined by

$$\mathcal{P}_{\mathrm{V}} := \frac{V_I}{V}, \tag{2}$$

where V_I denotes the volume of phase I and V denotes the total volume of a analyzed microstructure. The volume fraction plays an important role in microstructure reconstruction processes. However, higher order statistical measures were found to be important for the construction of SSRVEs in [1]. These include the spectral density, computed based on the discrete Fourier transformation of a microstructure by

$$\mathcal{P}_{\mathrm{SD}}(n_x, n_y, n_z) := \frac{1}{2\pi N_x N_y N_z} |\mathcal{F}(n_x, n_y, n_z)|^2 \tag{3}$$

with the discrete Fourier transformation given by

$$\mathcal{F}(n_x, n_y, n_z) := \sum_{k_x=1}^{N_x} \sum_{k_y=1}^{N_y} \sum_{k_z=1}^{N_z} \exp\left(2\pi \mathrm{i} \left(\frac{n_x k_x}{N_x} + \frac{n_x k_x}{N_x} + \frac{n_x k_x}{N_x}\right)\right) \chi(k_x, k_y, k_z). \tag{4}$$

The discrete data set is here considered by the coordinates k_x, k_y, k_z and its total size by N_x, N_y, N_z, whereas the frequency space is given by the coordinates n_x, n_y, n_z. The indicator function χ is defined as

$$\chi(k_x, k_y, k_z) := \begin{cases} 1 \text{ if point } x(k_x, k_y, k_z) \text{ lies in the inclusion phase} \\ 0 \text{ else.} \end{cases} \tag{5}$$

The spectral density captures periodicity information from the analyzed data set. Further information about a microstructure can be captured by analyzing its lineal-path function. It represents the probability that a line segment of a certain length and orientation is entirely located in one phase of the material, here the inclusion phase. The lineal-path function is then given by

$$\mathcal{P}_{\mathrm{LP}}(p, q, o) := \frac{1}{N_x N_y N_z} \sum_{m=1}^{N_x} \sum_{k=1}^{N_y} \sum_{l=1}^{N_z} \lambda(p, q, o) \tag{6}$$

with the indicator function

$$\lambda(p, q, o) := \begin{cases} 1 \text{ if } \overrightarrow{\mathbf{x_1 x_2}} \text{ is in the inclusion phase} \\ 0 \text{ else} \end{cases} \tag{7}$$

where the starting and ending point of the line segment are given by $\mathbf{x_1}(m, k, l)$ and $\mathbf{x_2}(p, q, o)$, respectively. Computing the lineal-path function is a rather costly task, which can be diminished by considering only a reduced set of line segments, thereby losing statistical information. Here, we analyze 1000 orientations of line segments distributed over the possible space of orientations of line segments. In order not to lose too much statistical information this high number of line orientations is required to realize a suitable trade-off of statistical information and reasonable computing time for the optimization problem.

From the theory of integral geometry, statistical measures based on Minkowski functionals, cf. [6], can be defined. Minkowski functionals are given as integrals of curvatures of smooth surfaces of a compact domain D_r with the boundary ∂D_r. In d-dimensional space, there exist $d+1$ scalar Minkowski functionals, which are the volume $\mathcal{W}_0(D_r)$, the area of bounding surface $\mathcal{W}_1(\partial D_r)$, the integral of mean curvature over the bounding surface $\mathcal{W}_2(\partial D_r)$ and the topological Euler-Poincaré index $\mathcal{W}_3(\partial D_r)$. These Minkowski functionals can be extended to tensorial measures using tensor products of the position vector $\mathbf{r}$ and normal vectors $\mathbf{n}$ of the boundary ∂D_r. It is evident that such Minkowski functionals defined in terms of position vectors need a reference point to which the vector is related, which thus causes a dependence of the Minkowski functional on the reference point. Tensorial Minkowski functionals based on the tensor product of the normal vectors $\mathbf{n} \otimes \mathbf{n}$ do not include this dependence. The associated Minkowski functionals differ by scalar prefactors and here we focus on

$$\mathcal{W}_1^{0,2}(\partial D_r) := \frac{1}{3}\int_{\partial D_r} \mathbf{n}\otimes\mathbf{n}\,\mathrm{dA} \tag{8}$$

with dA being an infinitesimal surface element on ∂D_r, cf. [6]. In contrast to the spectral density or lineal-path function, the Minkowski functional is computed for a compact domain and thus, in most cases, not for a complete microstructure, which may contain multiple compact domains. The Minkowski tensor can be understood as a descriptor for orientation distributions. Using the eigenvalues μ of the tensor, a scalar indicator for the anisotropy with respect to surface orientation can be defined as

$$\beta := \frac{\mu_{\min}}{\mu_{\max}} \in [0,1] \tag{9}$$

with $\mu_{\min}$ and $\mu_{\max}$ as the eigenvalues with minimal and maximal absolute value. A value of β equal to one is produced from an isotropic body and deviations from this value describe the degree of anisotropy, cf. [6]. Based on the decomposition of W into eigenvalues and respective eigenvectors v, another measure can be defined based on the orientation of the eigenvectors in space which are here described by two angles in spherical coordinates v(,). For ellipsoidal bodies, these eigenvectors are found to describe the orientation of the axis of the ellipsoid. Starting from this, we want to use the anisotropy measure and the eigenvectors v(,) as statistical descriptors of the inclusion phase in the microstructure. Since we obtain the measure for each inclusion separately, we compute histograms over all inclusions in the microstructure and divide by the number of inclusions to get a discrete probability distribution. In detail we consider a number of n_β categories c_{i_β}, $i_\beta = 1...n_\beta$ for β and define the probability $\mathcal{P}_{\mathrm{MA}}(i_\beta)$ of finding an inclusion with $\beta \in c_{i_\beta}$

$$\mathcal{P}_{\mathrm{MA}}(i_\beta) := \frac{1}{n_{\mathrm{incl}}}\sum_{m=1}^{n_{\mathrm{incl}}}\xi(i_\beta) \;\text{ with }\; \xi := \begin{cases} 1 \text{ if } \beta \in c_{i_\beta} \\ 0 \text{ else,} \end{cases} \tag{10}$$

as a measure for the anisotropy of the set of inclusions. For the eigenvectors, a classification into different histograms k is performed. We distinguish between four different cases, relating to the eigenvalue composition of the tensor: For three different eigenvalues we have three significant directions which are associated to the three eigenvectors. If two or three eigenvalues are equal, no distinct direction can be identified associated to these eigenvalues. Therefore, case (k=1,2,3) captures the existence of three distinct eigenvalues and the associated directions of eigenvectors in three separate histograms. For two equal eigenvalues the direction of the eigenvector to the associated third, distinct eigenvalue is captured in a histogram: case (k=4) denoting a distinct eigenvalue smaller than the other two and case (k=5) denoting a distinct eigenvalue larger than the other two equal eigenvalues. The case (k=6) of three equal eigenvalues does not provide any distinct direction of eigenvector and therefore the pure existence of an inclusion is recorded in the histogram. With this classification the histograms are defined as

$$\mathcal{P}_{\mathrm{MO}}(i_\theta, i_\varphi) := \frac{1}{n_{\mathrm{incl}}} \sum_{m=1}^{n_{\mathrm{incl}}} \xi(i_\theta, i_\varphi) \;\text{ with }\; \xi := \begin{cases} 1 \text{ if } \mathcal{D}_m \;\in\; B_k \\ 0 \text{ else,} \end{cases} \tag{11}$$

and the sets of inclusions for the individual cases, i.e.

$$\mathcal{B}_{k=1,2,3} := \{\mathcal{D}_m | \mu_1 > \mu_2 > \mu_3\} \tag{12}$$

$$\mathcal{B}_{k=4} := \{\mathcal{D}_m | \mu_1 = \mu_2 > \mu_3\} \tag{13}$$

$$\mathcal{B}_{k=5} := \{\mathcal{D}_m | \mu_1 > \mu_2 = \mu_3\} \tag{14}$$

$$\mathcal{B}_{k=6} := \{\mathcal{D}_m | \mu_1 = \mu_2 = \mu_3\}\,. \tag{15}$$

For $k = 1...5$ there are a number of $n_\theta \cdot n_\phi$ categories. This classification can be associated to properties for ellipsoidal shapes, where equal eigenvalues correspond to a spherical body. Here, the eigenvectors do not carry any information about specific axis. The case of two equal eigenvalues relates to a rotationally symmetric ellipsoid, where the radii on two axes are equal. It was found that the single eigenvalue in this case describes the orientation of the distinct orientation of the ellipsoid rotation axis. For a non rotationally symmetric ellipsoid, three distinct eigenvalues are found where all eigenvectors describe the orientation directions of the ellipsoid.

2.2 Proposed Method

The above described statistical measures are evaluated and compared in the following. Three sets of SSRVEs are constructed based on a least-square functional proposed in section 2.1. The errors calculated for the statistical measures are specified as

$$\mathcal{L}_{\mathrm{V/SD/LP}} := \omega_{\mathrm{V/SD/LP}} \frac{1}{N_{\mathrm{V/SD/LP}}} \sum_{i=1}^{N_{\mathrm{V/SD/LP}}} \left(\mathcal{P}^{\mathrm{real}}_{\mathrm{V/SD/LP},i} - \mathcal{P}^{\mathrm{SSRVE}}_{\mathrm{V/SD/LP},i}(\boldsymbol{\gamma})\right)^2 \tag{16}$$

and for the Minkowski measures as

$$\mathcal{L}_{\mathrm{MA/MO}} := \omega_{\mathrm{MA/MO}} \frac{1}{N_{\mathrm{MA/MO}}} \sum_{i=1}^{N_{\mathrm{ent}}} \left(\frac{V^{\mathrm{real}}_{\mathrm{MA/MO},i}}{V^{\mathrm{real}}} \mathcal{P}^{\mathrm{real}}_{\mathrm{MA/MO},i} - \frac{V^{\mathrm{SSRVE}}_{\mathrm{MA/MO},i}}{V^{\mathrm{SSRVE}}} \mathcal{P}^{\mathrm{SSRVE}}_{\mathrm{MA/MO},i}(\boldsymbol{\gamma}) \right)^2 \tag{17}$$

with $N_{\mathrm{V/SD/LP}}$ denoting the number of entries in the respective statistical measure and N_{ent} as the total number of entries in the histogram for MA and the total number of all entries in all histograms for MO for normalization purposes. $V^{\mathrm{real}}_{\mathrm{MA/MO},i}/V^{\mathrm{real}}$ and $V^{\mathrm{SSRVE}}_{\mathrm{MA/MO},i}/V^{\mathrm{SSRVE}}$ denote the volume ratio of all inclusions in the specific category with respect to the total volume of inclusions in the real microstructure and the SSRVE, respectively. The weighting factors are $\omega_{\mathrm{V}} = \frac{1}{\mathcal{P}^{\mathrm{real}}_{V}}$, $\omega_{\mathrm{SD}} = 1$, $\omega_{\mathrm{LP}} = 1000$, $\omega_{\mathrm{MA}} = 0.1$ and $\omega_{\mathrm{MO}} = 0.1$. These weighting factors were estimated by performing series of optimizations with different weighting factors and keeping the ones yielding the best performance. In the following sections, the complete least-square functionals for the construction of SSRVEs are presented.

3 COMPARATIVE STUDY

SSRVEs are constructed based on different combinations of statistical descriptors, which are presented in Section 2.1, namely

$$\begin{aligned} \mathcal{L}_1 &:= \mathcal{L}_{\mathrm{V}} + \mathcal{L}_{\mathrm{SD}} + \mathcal{L}_{\mathrm{LP}}, \\ \mathcal{L}_2 &:= \mathcal{L}_{\mathrm{V}} + \mathcal{L}_{\mathrm{SD}} + \mathcal{L}_{\mathrm{MA}}, \\ \mathcal{L}_3 &:= \mathcal{L}_{\mathrm{V}} + \mathcal{L}_{\mathrm{SD}} + \mathcal{L}_{\mathrm{MA}} + \mathcal{L}_{\mathrm{MO}}. \end{aligned} \tag{18}$$

Herein, SSRVEs with an artificial inclusion morphology are constructed, which consist of different numbers of ellipsoidal inclusions. In detail, for $\mathcal{L}_1$ SSRVEs with one, two and three inclusions are constructed to study the influence of inclusion number on the performance of the SSRVEs regarding a comparison of mechanical behavior with the target structure. Four virtual experiments, tension test in $x-$ and $z-$direction and shear tests in $xy-$ and $yx-$direction, are carried out for the target structure and the SSRVEs and an overall error measure $\tilde{r}$ is computed based on the deviation of the response for each virtual test by

$$\tilde{r} := \sqrt{\frac{1}{4}\tilde{r}_x^2 + \tilde{r}_z^2 + \tilde{r}_{xy}^2 + \tilde{r}_{yx}^2} \quad \text{with} \quad \tilde{r}_j := \sqrt{\frac{1}{n}\sum_{i=1}^{n}\left(r_j^i\right)^2} \quad \text{and} \quad r_j^i := \frac{\left(\sigma_{j,i}^{\mathrm{real}} - \sigma_{j,i}^{\mathrm{SSRVE}}\right)}{\sigma_{j,i}^{\mathrm{real}}} \tag{19}$$

where j denotes the respective virtual experiment and i represents the evaluation point. The results of the SSRVEs can be found in Table 1 and an illustration of the constructed artificial structures is shown in Figure 2.

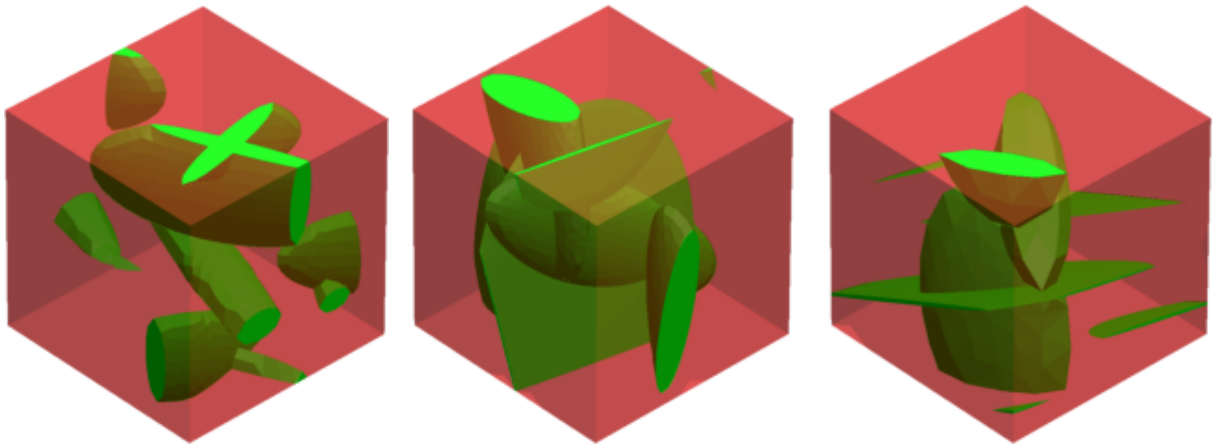

(a) (b) (c)

Figure 2: SSRVEs constructed based on (a) $\mathcal{L}_1$, (b) $\mathcal{L}_2$ and (c) $\mathcal{L}_3$

volume fraction, spectral density, lineal-path function: $\mathcal{L}_1 := \mathcal{L}_\mathrm{V} + \mathcal{L}_\mathrm{SD} + \mathcal{L}_\mathrm{LP}$										
	$\mathcal{L}_1/\ 10^{-2}$	$\mathcal{L}_V/\ 10^{-4}$	$\mathcal{L}_{SD}/\ 10^{-3}$	$\mathcal{L}_{LP}/\ 10^{-4}$	n_ele	$\tilde{r}_x$	$\tilde{r}_z$	$\tilde{r}_{xy}$	$\tilde{r}_{yx}$	$\tilde{r}$
1 Ell.	8.432	485.29	4.5	0.31	2851	5.3	4.6	5.5	5.5	5.24
2 Ell.	0.98	32.07	3.5	0.031	5015	0.5	3.6	4.5	4.5	3.66
3 Ell.	0.53	3.37	3.3	0.017	18835	0.5	1.8	1.6	1.5	1.44
volume fraction, spectral density, Minkowski anisotropy: $\mathcal{L}_2 := \mathcal{L}_\mathrm{V} + \mathcal{L}_\mathrm{SD} + \mathcal{L}_\mathrm{MA}$										
	$\mathcal{L}_2/\ 10^{-4}$	$\mathcal{L}_V/\ 10^{-9}$	$\mathcal{L}_{SD}/\ 10^{-4}$	$\mathcal{L}_{MA}/\ 10^{-4}$	n_ele	$\tilde{r}_x$	$\tilde{r}_z$	$\tilde{r}_{xy}$	$\tilde{r}_{yx}$	$\tilde{r}$
3 Ell.	2.52	2.75	1.96	5.6	37687	2.5	5.4	5.2	5.2	4.73
volume fraction, spectral density, Minkowski anisotropy and orientation: $\mathcal{L}_3 := \mathcal{L}_\mathrm{V} + \mathcal{L}_\mathrm{SD} + \mathcal{L}_\mathrm{MA} + \mathcal{L}_\mathrm{MO}$										
	$\mathcal{L}_3/\ 10^{-4}$	$\mathcal{L}_V/\ 10^{-5}$	$\mathcal{L}_{SD}/\ 10^{-3}$	$\mathcal{L}_{MA}/\ 10^{-4}$	$\mathcal{L}_{MO}/\ 10^{-3}$	n_ele	$\tilde{r}_x$	$\tilde{r}_z$	$\tilde{r}_{xy}$	$\tilde{r}_{yx}$	$\tilde{r}$
3 Ell.	7.87	1.98	5.62	1.11	1.94	20427	0.7	2.6	0.4	0.4	1.38

Table 1: Error of mechanical tests in % and error in statistical measures for SSRVEs constructed by $\mathcal{L}_1$, $\mathcal{L}_2$ and $\mathcal{L}_3$.

It can be seen that with an increase of complexity of inclusion morphology, the error in the statistical measures $\mathcal{L}_1$ decreases as well. Furthermore, a decrease can be also seen in the overall mechanical error. For a SSRVE with three inclusions an error of 1.44% is observed, thus it can be regarded as a suitable substitute for the real microstructure.
In a next step, the performance of anisotropy and orientation measure from the Minkowski functional is analyzed with respect to the influence on the error in mechanical tests compared with the target structure. They replace the computationally expensive lineal-path function in the least-square functional. SSRVEs with three ellipsoidal inclusions are constructed based on $\mathcal{L}_2$, using only the anisotropy measure from $\mathcal{W}_1^{0,2}$, and $\mathcal{L}_3$, incorporating both, anisotropy and orientation measure from $\mathcal{W}_1^{0,2}$. The results are compared with the SSRVE with three inclusions from $\mathcal{L}_1$, see Table 1. A plot of the error over strain of the mechanical tests is also shown in Figure 3. Comparing the overall mechanical error, it can be seen that the anisotropy measure computed based on the Minkowski tensor is not able to serve as a suitable replacement for the lineal-path function because of the higher overall mechanical error. For the SSRVE constructed using additionally the orientation measure, we observe an error of similar value in the mechanical comparison and thus we can regard this SSRVE as a suitable representation of the real microstructure as well. Furthermore, the optimization time of $\mathcal{L}_1$ can be reduced by a factor of 6.5 by using $\mathcal{L}_2$ instead, i.e. replacing the lineal-path function by the anisotropy and orientation measure based on the Minkowski functional $\mathcal{W}_1^{0,2}$.

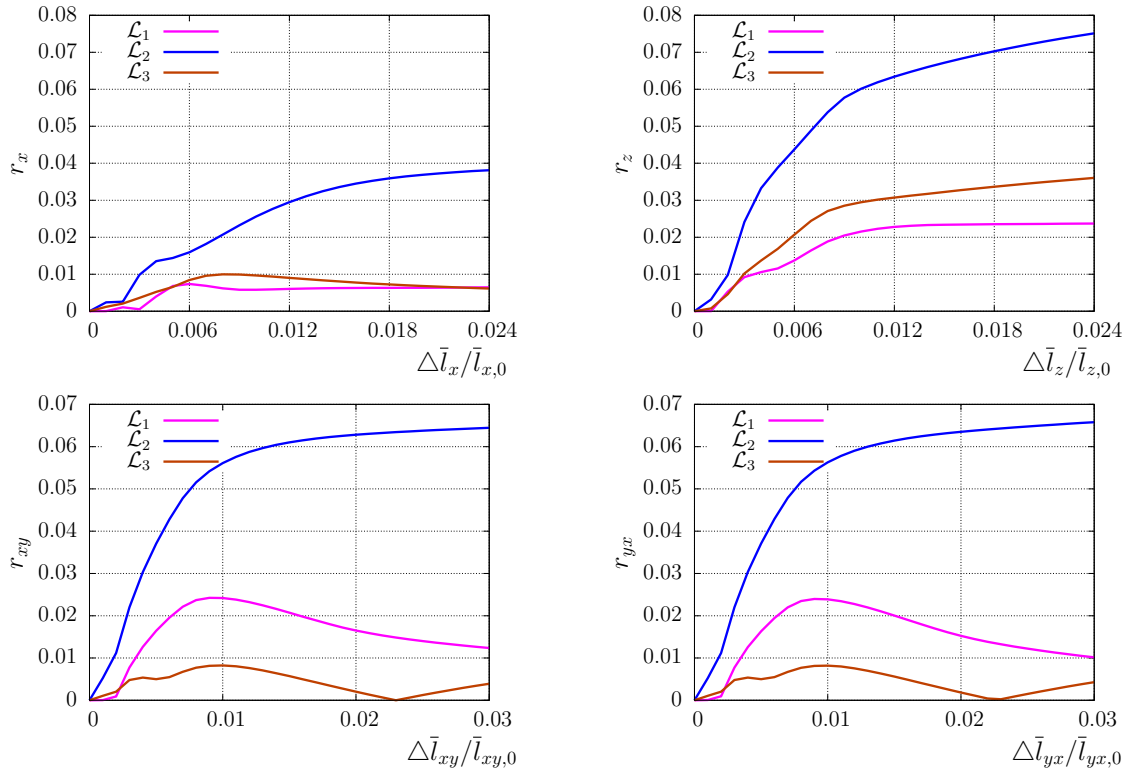

Figure 3: Mechanical error analysis of SSRVEs based on $\mathcal{L}_1$, $\mathcal{L}_2$ and $\mathcal{L}_3$: tension test x_1 (upper left), tension test x_3 (upper right), shear test xy (lower left) and shear test yx (lower right)

4 CONCLUSION

A method for the construction of 3D SSRVEs was proposed and applied using different sets of statistical measures. From the presented results, a lower error in the statistical measures and also in the mechanical error compared to the target structure were seen for an increased complexity of the inclusion morphology. The SSRVE based on the volume fraction, spectral density, anisotropy measure and orientation measure obtained from a Minkowski functional leads to similar results regarding the mechanical response compared with the target structure as the SSRVE based on volume fraction, spectral density and lineal-path function while further providing a speedup in the optimization process. Solely using the Minkowski anisotropy measure instead of the lineal-path function turned out to be not sufficient.

Acknowledgement: Financial funding by the DFG-Research group FOR 797 - P8, project no. SCHR570/8-2, is acknowledged. We appreciate the kind support of Prof. D. Raabe (Max-Planck Institut für Eisenforschung in Düsseldorf) for providing the EBSD/FIB measurements.

REFERENCES

[1] Balzani, D., Brands, D., Schröder, J., Carstensen, C., Sensitivity analysis of statistical measures for the reconstruction of microstructures based on the minimization of generalized least-square functionals. *Technische Mechanik*(2010), **30**:297–315.

[2] Balzani, D., Scheunemann, L., Brands, D., Schröder, J. Construction of 3D statistically similar RVEs for dual-phase steel microstructures. In *XII International Conference on Computational Plasticity. Fundamentals and Applications.* September 3-5, Barcelona, Spain

[3] Miehe, C., Schröder, J., Schotte, J. Computational homogenization analysis in finite plasticity. Simulation of texture development in polycrystalline materials. *Comp. Meth. App. Mech. Eng.* (1999) **171**:387–418.

[4] Ohser, J., Mücklich, F. *Statistical Analysis of microstructures in materials science.* J. Wiley & Sons. (2000)

[5] Schröder, J., Balzani, D., Brands, D. Approximation of random microstructures by periodic statistically similar representative volume elements based on lineal-path functions. *Arch. Appl. Mech.* (2011) **81**:975–997.

[6] Schröder-Turk, G. E., Mickel, W., Kapfer, S. C., Klatt, M. A., Schaller, F. M., Hoffmann, M. J. F., Kleppmann, N., Armstrong, P., Inayat, A., Hug, D., Reichelsdorfer, M., Peukert, W., Schwieger, W., Mecke, K. Minkowski Tensor Shape Analysis of Cellular, Granular and Porous Structures. *Advanced Materials* (2011), **23**:2535–2533.

[7] Yeong, C. L. Y., Torquato, S. Reconstructing random media. *Physical Review E.* (1998) **57**:495–506.